Photoexcitation dynamics in polyconjugated molecules

Sergei Tretiak*, Avadh Saxena, Richard L. Martin, and Alan R. Bishop

Theoretical Division, Los Alamos National Laboratory, Los Alamos, New Mexico 87545

Abstract

π-conjugated polymers have become an important class of materials for electronic devices. Design of these devices requires understanding such processes as photochemical reactions, spatial dynamics of photoexcitations, and energy and charge transport, which in turn involve complex coupled electron-vibrational dynamics. Here, we study photoexcitation dynamics in of several conjugated polymers using a new quantum-chemical method suitable for the simulation of excited state molecular dynamics in extended molecular systems with sizes up to hundreds of atoms. Calculated excited state energies and parameters of molecular adiabatic surfaces characterize the coupled dynamics of vibrational and electronic degrees of freedom. The analysis identifies the specific torsional and bond-stretching nuclear motions that dominate the excited state relaxation and lead to self-localized excitations in poly(p-phenylene vinylene) (PPV) oligomers. The simulations reveal formation of a self-localized vibronic excitation ("breather" or multiquanta bound state) with typical period of 34 fs in polyenes. Possible correlated electronic and vibrational spectroscopic signatures of photoexcited breathers are predicted, and generalizations to energy localization in complex macromolecules are discussed. This computational approach is an inexpensive and numerically efficient method of computing molecular excited state adiabatic surfaces and modeling femto-to-pico second time-dependent photoexcitation processes along chosen trajectories.

* Corresponding author. E-mail: serg@lanl.gov

Introduction

Light emitting conjugated polymers are of interest both for their broad technological applications and because they are model systems to gain fundamental understanding of the properties of soft organic and biological matter (1,2,3). Almost every photochemical, photophysical or spectroscopic process in these materials involve dynamics of photoexcited states (4,5) and, for this reason, its theoretical characterization has immediate technological implications and offers valuable insight into the nature and behavior of excitations in soft materials (2,3). However, the theoretical description of these molecular systems is challenging because of electronic correlation effects and strong electron-lattice interactions (6,7). Development of powerful computers and versatile program packages leads to the growing importance of quantum chemistry for the understanding underlying fundamental electronic phenomena and for providing accurate predictions of relevant observables in organic matters. Computing molecular vertical excitation energies and polarizabilities has addressed some structure-function issues for predicting structures with desired optical properties and modeling of spectroscopic probes (6,7). However, coupled electron-vibrational dynamics becomes vital for understanding and simulating such processes as time-dependent dynamics of photoexcitations in the bulk polymeric materials, formation of excitons, polarons, and other quasiparticles which govern spectroscopical, photo-optical, energy and charge transport properties of the media. Calculation of excited states is still challenging, since it requires an expensive multiconfiguration representation. This high demand of computational resources has limited excited state surface calculations to small molecules (5-10 atoms) (8) or to single-point computations (6,7), which compute a snapshot of the excited state structure for a given molecular geometry.

In this article we analyze excited state time-dependent processes in large molecular systems based on poly(p-phenylene vinylene) and polyacetylene structures using the quantum-chemical approach. Our excited state molecular dynamics (ESMD) method (9,10) satisfactory accounts for electronic correlations and allows us to model femto-to-pico second dynamics of quite large (100-150 atoms) molecular systems taking into account all (3N-6) vibrational degrees of freedom (N being the number of atoms in the molecule).

Computational approach

We have recently developed a theoretical approach which permits investigation of excited state dynamics, visualizion of electronic/vibronic processes on the excited state manifold, and guidance of rational synthesis of materials with properties tailored to specific optoelectronic applications (9,10). The method is based on the random phase approximation combined with semiempirical Hamiltonians (7). It provides a relatively inexpensive procedure for following excited state molecular dynamics. The computations propagate the classical Newtonian equation of motion

$$[1] \qquad M_a \frac{\partial^2 \mathrm{q}_a}{\partial t^2} + \beta \frac{\partial \mathrm{q}_a}{\partial t} = F_a = -\frac{\partial E_\mathrm{e}}{\partial \mathrm{q}_a}$$

along the trajectory on the excited state molecular potential surface. Here $\mathbf{q}_\alpha$ represent 3N-6 molecular vibrational degrees of freedom and E_e is the excited state potential energy (see Fig. 1). The forces F_α in the right-hand side of this equation are computed with the quantum chemical collective electronic oscillator (CEO) algorithm combined with semiempirical Hamiltonian models (7). The computations allow us to follow excited state molecular dynamics in the gas phase with vanishing damping ($\beta=0$) or motion in a viscous liquid ($\beta\neq0$). The latter leads us to the excited state optimal geometry, as illustrated in Fig. 1.

We used the Austin Model 1 (AM1) Hamiltonian (11) for all calculations presented in this paper. AM1 has been specifically parameterized to reproduce ground state properties (such as chemical energy, geometry, dipole moment, etc.) in a variety of molecules (11). In addition, this model provides a reasonable accuracy for excited state properties in combination with the Random Phase Approximation (12). Standard Verlet-type numerical integration (13) has been used to propagate [1] in time. At present the algorithm computes forces F_α in the excited state with numerical differentiation, as opposed to more efficient analytical derivative technique which is also possible within the present approach (14). However, implementation of the direct inversion iterative subspace algorithm for calculating the ground state energy E_g, and very efficient Davidson (7,15) diagonalization techniques for computing excitation frequencies Ω, makes it possible to follow picosecond dynamics of quite large (100-200 atoms) molecular systems taking into account all (3N-6) vibrational degrees of freedom.

Conformational excited state dynamics in poly(p-phenylene vinylene)

We have investigated excited state geometries in oligomers of various lengths (n=2-14) of PPV, which is an important material for electronic device applications (2,3). The study focuses on the lowest singlet excited state $1B_u$ of PPV which plays a major role in absorption, photoluminescence and carrier transport in conjugated systems (6,7). Fig. 2 shows the variation with oligomer size of the vertical absorption Ω_A (computed at the ground state optimal geometry) and fluorescence Ω_F (calculated at the excited state optimal geometry) frequencies, Stokes shift and vibrational reorganization energy for the $1B_u$ transition. The energies of absorption and fluorescence, as expected, are red-shifted with increasing oligomer length, saturating to 2.65 and 2.4 eV for long chains, respectively, which compares well with the corresponding experimental values 2.7 and 2.4 eV (16). The vibrational reorganization energy also decreases with increasing of the chain length, albeit at a slower rate.

To rationalize these trends in spectroscopic observables, we first examine structural changes when going from the ground to the excited state equilibrium geometries. The ground state structure of PPV is not planar. The energy profile is very shallow with respect to the librational motion; weak perturbations, such as impurities and intermolecular interactions, may lead to significant torsional disorder. In particular, interaction of the σ-bonds results in a structure with the neighboring phenyl-vinyl twisted by ~ 15^o in the AM1 geometry, which agrees with x-ray structures reported for $(PPV)_5$

crystals (17). The situation is very different for the excited state. Here the energy profile is no longer shallow with respect to the torsional motion and has its global minimum at a planar structure. An important feature of a conjugated oligomer's geometry is the bond length alternation due to the non-constant distribution of the π electrons over the bonds (Peierls distortion) (6,7). The bond length alternation parameter in the adjacent vinylene linkages is constant along the chain for the ground state geometry, and noticeably reduced in the middle of the molecule for the excited state geometry.

To investigate how these geometrical changes are connected with the underlying photoinduced dynamics of electronic charges, we use a two-dimensional real-space analysis of transition densities, representing the electronic transition between the ground state and an electronically excited state (7). Photoexcitation creates an electron-hole pair or an exciton by promoting an electron from an occupied orbital to an unoccupied orbital. Each element of the transition density reflects the dynamics of this exciton projected on a pair of atomic orbitals given by its indices.

Plots of transition density matrices in PPV oligomers are shown in Fig. 3. Each plot depicts probabilities of an electron moving from one molecular position (horizontal axis) to another (vertical axis), under a transition from the ground state to the $1B_u$ excited state (7). An electron-hole pair initially created by an absorbed photon (``hot exciton'') is entirely delocalized in the smallest oligomer $(PPV)_2$ and confined by the molecular ends (Fig. 3A). For longer oligomers (Figs. 3C-D), the electron-hole pair is also delocalized over the whole chain (diagonal in the plot) but is not confined by the molecular ends. The exciton size (maximal distance between electron and hole) is 4 repeat units (largest off-diagonal extent of the nonzero matrix area). This electronic excitation then relaxes along the excited state potential surface into a ``cold exciton'', which may decay radiatively back to the ground state (fluorescence). Figs. 3A'-D' display corresponding transition densities computed in the excited state geometry. Transition densities in the ground and excited state geometries for the smaller oligomers $(PPV)_2$ and $(PPV)_5$, being in the confined regime, are very similar, as seen from comparing plots A and A' (B and B'). However, the effect of the excited state geometry relaxation is clearly observed for longer oligomers ($(PPV)_{10}$ and $(PPV)_{14}$) by comparing plots C and C' (D and D'): the exciton, initially diagonally delocalized along the whole molecule, becomes localized in the center of the chain. We notice that relaxed excitations in $(PPV)_{10}$ (plot C') and $(PPV)_{14}$ (plot D') are virtually identical, with a diagonal size of about 6 repeat units in the middle of the molecule, consistent with the region of reduced bond-length alternation. This suggests exciton self-trapping at the center of the chain by structural relaxation (18).

Photoexcited breathers in conjugated polyenes

We next investigate the formation of photoexcited *breathers* i.e., multiquanta vibronic states in polyacetylene (inset in Fig. 4). A breather is a dynamic state representing a spatially localized, time-persistent nonlinear excitation. Extensive studies based on simple Hamiltonian models predicted the formation of breather-like states in polyenes after either photoexcitation or electronic ground state perturbations of sufficient energy (19,20). However, it took almost two decades to develop ultrafast sub 5 fs experimental spectroscopic techniques to monitor real-time vibronic dynamics of conjugated polymers which may support the existence of breathers (4). Our results reproduce all the essential features of the early studies and provide quantitative information necessary for modeling a variety of spectroscopic techniques. This allows us to connect these simulations with recent experiments and to predict additional spectroscopic signatures of breathers.

To analyze excited state dynamics of cis-polyacetylene, we calculate oligomers (with free boundary conditions) long enough (inset in Fig. 4) to mimic the infinite chain limit and up to a 1 ps timescale. To monitor the vibrational dynamics we focus on the bond-length alternation parameter (6,7), which reflects strong coupling to the electronic system. To follow the electronic dynamics we further use a real-space, two-dimensional representation of the transition density matrices.

The left column of Fig.4 shows the variation of bond-length alternation parameter, and the right column of Fig. 4 displays the correspondent transition densities at specific times up to 100 fs. At the moment of photoexcitation (t=0) the molecule in the ground state has a constant dimerization

(0.095 A). The effects from the molecular ends are small and local. Therefore, upon the photoexcitation, the exciton created is initially delocalized along the entire chain (Fig. 4, t=0). Due to strong electron-phonon coupling an exciton rapidly distorts the lattice in the middle of the chain (Fig. 4, t=16 fs) and localizes in this region on the timescale of ~20 fs. When an exciton distorts the lattice, dynamical vibrational excitations (phonons) are created, appearing as waves in the bond-length alternation at the edges of the exciton potential well (Fig. 4, t=44 fs). The subsequent dynamics can be qualitatively described as follows: the phonon "waves" propagate in opposite derections, reflect from the chain ends, and meet in the middle of the chain (e.g. Fig. 4, t=100 fs) pulling an exciton out of its well and delocalizing the excitation (e.g. density in Fig. 4, t=100 fs). The exciton, in turn, attempts to re-localize, creating more phonons, i.e. the energy is exchanging between electronic and vibrational degrees of freedom. This variation of diagonal delocalization is a characteristic "breathing" pattern with period of ~34 fs.

The characteristic timescales of this electron-vibrational motion appear on the power spectra of all spectroscopic observables (transition frequencies, transition dipoles, and polarizabilities) which contain frequency components with periods of ~18, ~34, and ~70 fs. Only the ~18 fs harmonic is related to the C=C stretching vibrational normal mode (ω=1826 cm^{-1}), whereas the other two harmonics are not associated with the vibrational spectrum, with ~34 fs being the breather excitation. We observe that the breather component has the strongest signature in transition dipoles and oscillator strengths, whereas energy variables (such as transition frequencies) are dominated by vibrational mode frequency components (in particular the C=C stretching). The magnitudes of the transient absorption spectra are related to the respective transition dipole moments and, therefore, contain the breather vibrational component in their power spectra, which should allow identification of breather excitations experimentally (4). The breather believed to be observed in the experiment has a short lifetime of about 50 fs (4). We can understand this dissipation by recalling that in our simulations phonon waves reflect from the molecular ends without vibrational energy loss. In real samples the phonons will be scattered on the defects which limit the conjugated segment and only a fraction of their energy will return back to sustain the breather. Interchain interaction could enhance these dissipative processes even further. Stronger defects will be less transparent for phonons. Therefore, we expect that breathers will have longer lifetimes in the defected samples. To confirm this scenario, additional simulations showed that, in the case of weak chemical defects, the energy dissipates on the timescale of ~70 fs, whereas in the chain with stronger defects the breather persists up to ~200 fs.

Conclusion

Strong nonlinear coupling among electronic and vibrational degrees of freedom leads to a complex spatially localized photoexcited vibronic dynamic simulation which is a distinctive property of conjugated polymers. Our photoexcitation dynamics shows several characteristic features i) an excitation moves to the largest conjugated segment of the polymer chain (where it has the lowest electronic energy), since bandgaps decrease with increasing chain length; ii) an exciton creates phonon excitations and significant local distortions of the lattice. These phonons form a complex nonlinear localized vibrational excitation (breather) which cannot be associated with any specific single linear vibrational normal mode. The subsequent dynamics is spatially localized and appears as an exchange of energy between an exciton and a breather; iii) the breather excitation has distinct spectroscopic signatures in the power spectra of all spectroscopic observables, iv) finally, due to dissipation processes, photoexcitation relaxes into a self-trapped exciton creating a localized lattice distortion. We expect that these processes are typical for conjugated materials featuring strong electron-phonon coupling, including disordered nanomolecules. Development of ultrafast sub-femtosecond spectroscopic techniques and efficient quantum-chemical approaches allows monitoring of time-dependent vibronic processes. This opens the way to more deeply understand a number of photochemical, time-dependent spectroscopic and carrier transport processes in electronically-active soft and biological nanoscale matter.

Acknowledgements

This work was performed under the auspices of the US Department of Energy and the LDRD program at LANL.

References

(1) A. J. Heeger, *Rev. Mod. Phys.*, **73**, 681 (2001).
(2) R. H. Friend, *Pure Appl. Chem.*, **73**, 425 (2001).
(3) M. A. Baldo, M. E. Thompson, and S. R. Forrest, *Nature*, **403**, 750 (2000).
(4) S. Adachi, V. M. Kobryanskii, and T. Kobayashi, *Phys. Rev. Lett.*, **89**, 027401 (2002).
(5) G. Lanzani, G. Cerullo, C. Brabec, N. S. Sariciftci, *Phys. Rev. Lett.*, **90**, 047402 (2003).
(6) J. L. Bredas, J. Cornil, D. Beljonne, D. A. dos Santos, and Z. Shuai, *Acc. Chem. Res.*, **32**, 267 (1999).
(7) S. Tretiak, and S. Mukamel, *Chem. Rev.*, **102**, 3171 (2002).
(8) M. Ben-Nun, F. Molnar, K. Schulten, and T. J. Martinez, *Proc. Nat. Acad. Sci. USA*, **99,** 1769 (2002).
(9) S. Tretiak, R. L. Martin, A. Saxena, and A. R. Bishop, *Phys. Rev. Lett.*, **89**, 97402 (2002).
(10) S. Tretiak, R. L. Martin, A. Saxena, and A. R. Bishop, *Proc. Nat. Acad. Sci. USA*, **100,** 2185 (2003).
(11) M. J. S. Dewar, E. G. Zoebisch, E. F. Healy, and J. J. P. Stewart, *J. Am. Chem. Soc.*, **107**, 3902 (1985).
(12) S. Tretiak, R. L. Martin, A. Saxena, and A. R. Bishop, *J. Chem. Phys.*, **115**, 699 (2001).
(13) M. P. Allen and D. J. Tildesley, *Computer Simulation of Liquids*, (Clarendon Press, Oxford, 1987).
(14) F. Furche and R. Ahlrichs, *J. Chem. Phys.*, **117**, 7433 (2002).
(15) E. R. Davidson, *J. Comp. Phys.*, **117**, 87 (1975).
(16) S. J. Martin, H. Mellor, D. D. C. Bradley, P. L. Burn, *Opt. Materials*, **9**, 88 (1998).
(17) P. F. van Hutten and J. Wildeman and A. Meetsma and G. Hadziioannou, *J. Am. Chem. Soc.*, **121**, 5910 (1999).
(18) A. J. Heeger, S. Kivelson, J. R. Schrieffer, and W. P. Su, *Rev. Mod. Phys.*, **60**, 781 (1988).
(19) A. R. Bishop, D. K. Campbell, P. S. Lomdahl, B. Horovitz, and S. R. Phillpot, S.R., *Phys. Rev. Lett.*, **52**, 671 (1984).
(20) J. Takimoto and M. Sasai, *Phys. Rev. B*, **39**, 8511 (1989).

Figure captions:

Figure 1: Schematic representation of ESMD propagation. Quantities of interest are excited state energy $E_e(\mathbf{q})$, as a function of nuclear coordinates $\mathbf{q}$, displacements Δ, curvatures ω_e/ω_g, vibrational reorganization energy ΔE_v, vertical absorption Ω_A and fluorescence Ω_F frequencies.

Figure 2: Calculated variation of vertical absorption Ω_A and fluorescence Ω_F frequencies, Stokes shift Ω_A-Ω_F and vibrational reorganization energy ΔE_v with the number of repeat units in the PPV chain.

Figure 3: Contour plots of transition density matrices. (**A**)-(**D**) represent transition from the ground state (equilibrium geometry) to the lowest excited state in $(PPV)_2$, $(PPV)_5$, $(PPV)_{10}$, and $(PPV)_{14}$ oligomers, respectively, and correspond to vertical absorption. (**A'**)-(**D'**) are the same quantities as in (**A**) - (**D**), but computed at the excited state equilibrium geometries, and correspond to vertical fluorescence. The axes labels represent the number of repeat units, and the color code is shown on the right.

Figure 4: Simulation of photoexcited breather in conjugated polyenes. An absorbed quantum of light initiates coupled nonlinear dynamics of collective electronic (electron and hole) and lattice (breather) excitations. Left column shows the variation of bond-length alternation parameter along the polymer chain (i.e. phonon waves related to the lattice motion). Right column displays contour plots of transition densities describing electron-hole motion (coherent breathing) after photoexcitation. The axes labels represent the carbon atoms, and the color code is shown in Fig. 3.

Figure 1

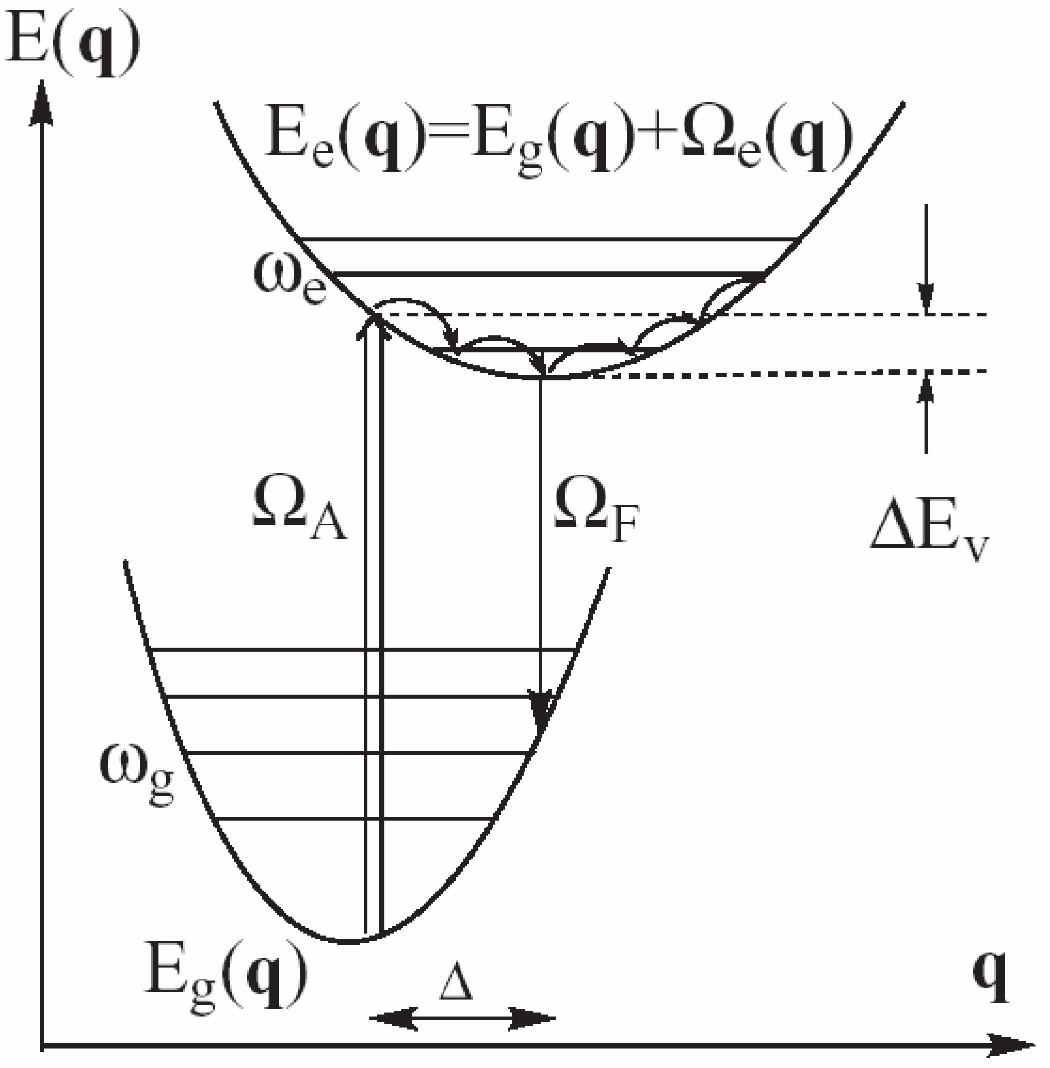

Figure 2

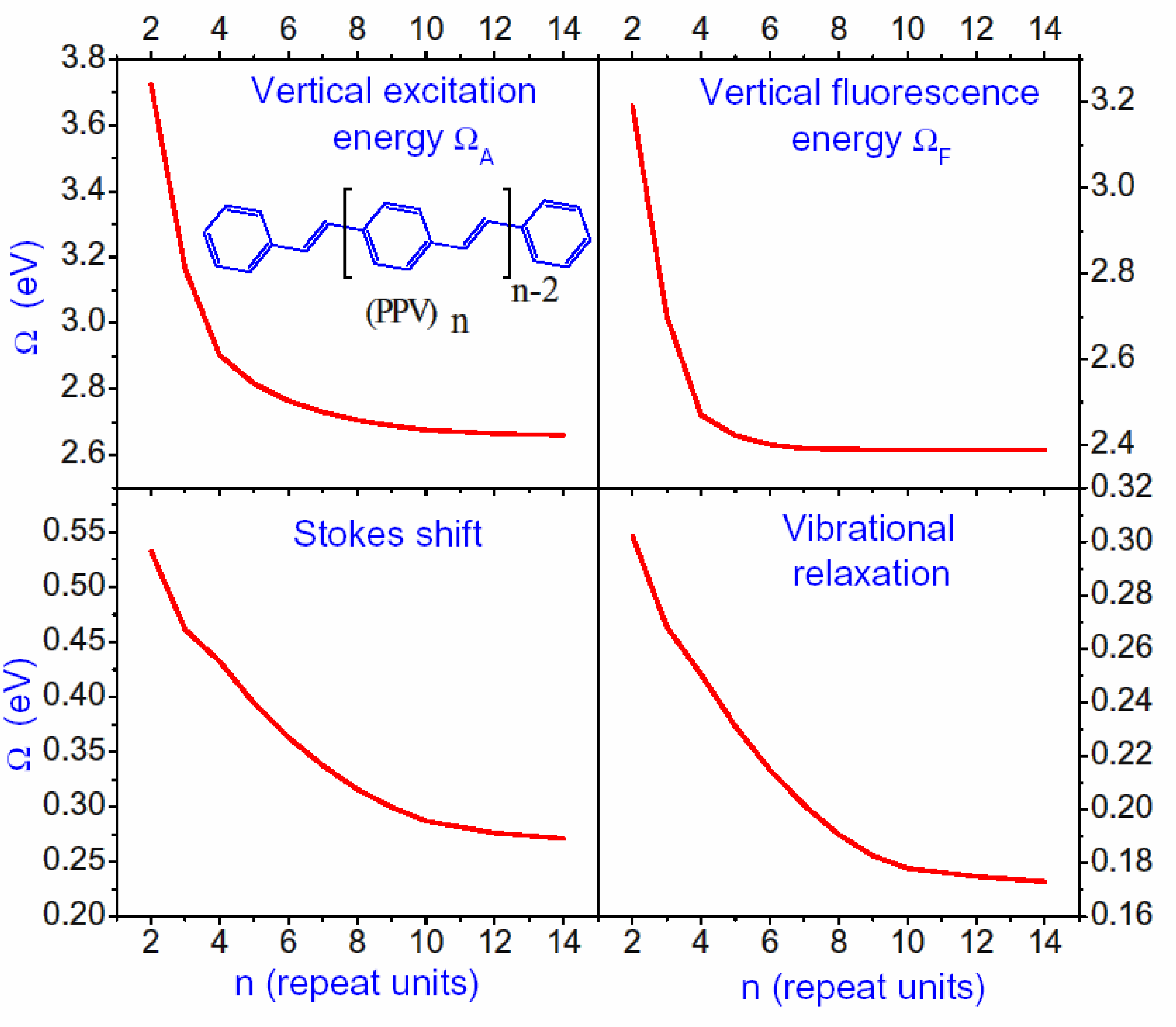

Vertical excitation energy Ω_A
Vertical fluorescence energy Ω_F
Stokes shift
Vibrational relaxation
(PPV) n
n-2
Ω (eV)
Ω (eV)
n (repeat units)
n (repeat units)
2
4
6
8
10
12
14
3.8
3.6
3.4
3.2
3.0
2.8
2.6
3.2
3.0
2.8
2.6
2.4
0.55
0.50
0.45
0.40
0.35
0.30
0.25
0.20
0.32
0.30
0.28
0.26
0.24
0.22
0.20
0.18
0.16

Figure 3

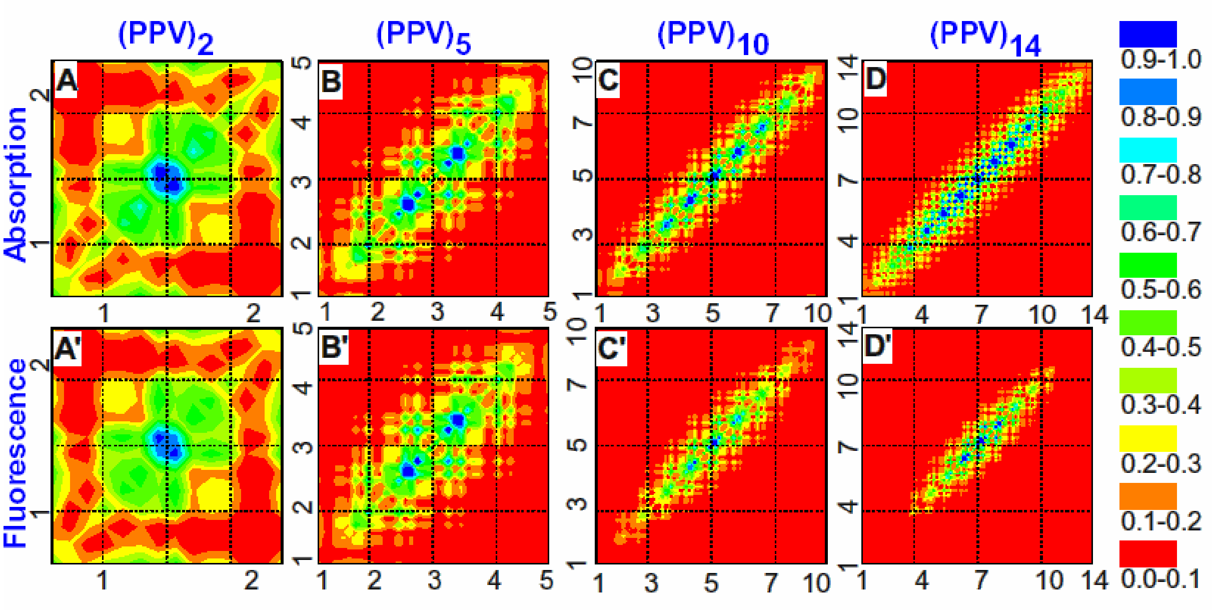
(PPV)$_2$
(PPV)$_5$
(PPV)$_{10}$
(PPV)$_{14}$
Absorption
Fluorescence
A
B
C
D
A'
B'
C'
D'
1
2
1
2
3
4
5
1
3
5
7
10
1
4
7
10
14
0.9-1.0
0.8-0.9
0.7-0.8
0.6-0.7
0.5-0.6
0.4-0.5
0.3-0.4
0.2-0.3
0.1-0.2
0.0-0.1

Figure 4

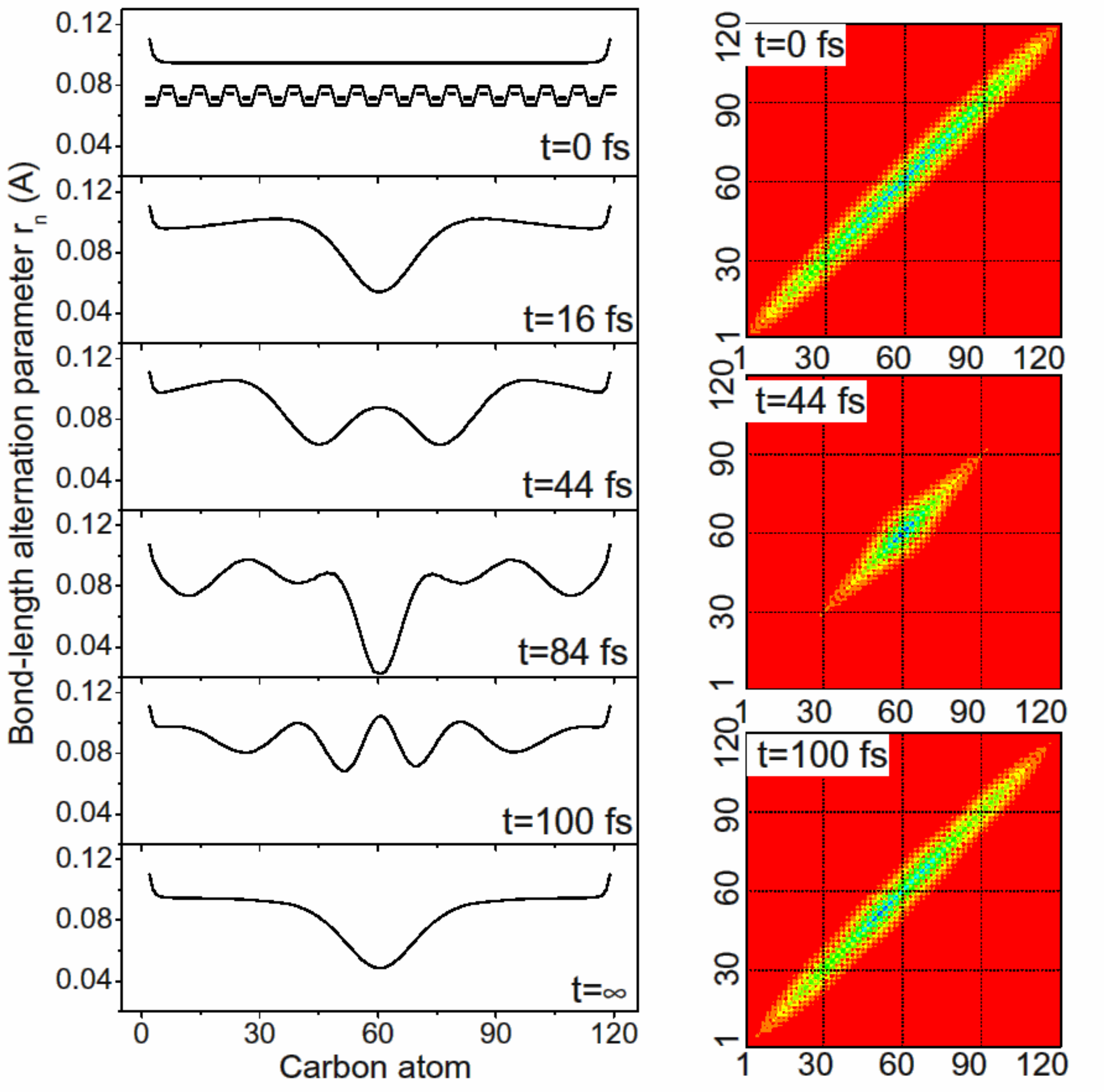
Bond-length alternation parameter r_n (A)
0.12
0.08
0.04
t=0 fs
t=16 fs
t=44 fs
t=84 fs
t=100 fs
t=∞
0
30
60
90
120
Carbon atom
t=0 fs
t=44 fs
t=100 fs
1
30
60
90
120